J|A|C|S COMMUNICATIONS

Published on Web 12/10/2010

Water-Soluble Peptide-Coated Nanoparticles: Control of the Helix Structure and Enhanced Differential Binding to Immune Cells

Iria M. Rio-Echevarria,[†,‡] Regina Tavano,[§,||] Valerio Causin,[†] Emanuele Papini,[§,||] Fabrizio Mancin,[†,*] and Alessandro Moretto[†,*]

Dipartimento di Scienze Chimiche, Università di Padova, via Marzolo 1, 35131 Padova, Italy, Dipartimento di Biologia, Università di Padova, via U. Bassi 58/B, 35131 Padova, Italy, Dipartimento di Scienze Biomediche Sperimentali, Università di Padova, via U. Bassi 58/B, 35131 Padova, Italy, and Centro di Ricerca Interdipartimentale per le Biotecnologie Innovative (CRIBI), Università di Padova, via U. Bassi 58/B, 35131 Padova, Italy

Received August 22, 2010; E-mail: fabrizio.mancin@unipd.it; alessandro.moretto.1@unipd.it

Abstract: The stabilizing action of C^{α}-tetrasubstituted α-amino acids inserted into a sequence of short peptides allowed for the first time the preparation of water-soluble nanoparticles of different materials coated with a helix-structured undecapeptide. This peptide coating strongly favors nanoparticle uptake by human immune system cells.

Self-organization of simple building blocks to generate large structures is an intriguing strategy for the formation of complex systems.[1] In particular, monolayer-protected nanoparticles rank among the top representatives of such an approach.[2] In their synthesis, a mixture of molecular precursors is converted by the addition of appropriate reagents into a collection of monodisperse and well-organized objects wherein an inorganic core is coated with a tightly packed three-dimensional (3D) monolayer of organic species.[3] It is not surprising that in the past decade such organization has been exploited for several important applications, ranging from catalysis[4] and sensing[5] to energy conversion,[6] development of new materials,[7] and biomedicine.[8]

A target that has been extensively addressed over the years is the preparation of water-soluble nanoparticles coated with peptides that have a defined helix secondary structure. Viewed from the outside, such nanoparticles closely resemble artificial globular proteins, where the biocompatibility of the coating, the chiral space organization, and the functional group crowding could pave the way for the realization of complex functional systems.[9] To date, such a goal has been frustrated by the complex interligand interactions that can be established between spatially close peptide chains.[10] These interactions strongly affect the monolayer structure as well as the nanoparticle solubility. As a result, the few examples of similar systems reported to date are soluble in nonaqueous solvents only.[11]

To address this problem, we turned our attention to peptides containing α-aminoisobutyric acid (Aib). C^{α}-tetrasubstituted α-amino acids are known to stabilize helix structures, even in short peptides,[12] and we reasoned that they could help to maintain this structure even after nanoparticle grafting[11] and exposure to aqueous solutions. For this study, we selected the water-soluble undecapeptide H-Ala_3-(Aib-Ala)$_4$-OMe (OMe = methoxy), which is known to form a helix in solution[13] and is characterized by a free

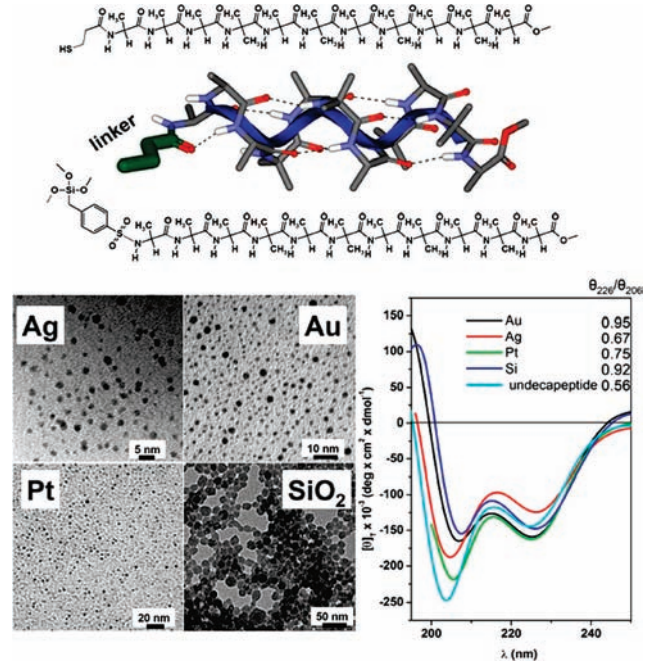

Figure 1. (top) Chemical structures of the nanoparticle-protecting peptides **1** (upper structure) and **2** (lower structure). (bottom) Representative TEM micrographs (left) and CD spectra (right) of **1** and undecapeptide-coated Au, Ag, Pt, and ormosil (Si) nanoparticles (see the SI for the CD spectrum of **2**).

N-terminal amino group that allows easy conjugation of the peptide with nanoparticle anchoring moieties such as trityl (Trt)-protected mercaptopropionic acid (for metal nanoparticles; peptide **1** in Figure 1) or 2-(4-chlorosulfonylphenyl)ethyltrimethoxysilane (for silica nanoparticles; peptide **2** in Figure 1) via standard solution chemistries.

Significantly, these conjugates are water-soluble, like the parent peptide itself, and the helix structure is maintained even in this solvent. Moreover, the peptide conjugates work as universal nanoparticle capping agents, allowing for the straightforward preparation of different peptide-protected nanoparticles with gold, silver, platinum, and organic-modified silica (ormosil) cores using standard protocols [Figure 1 and Figure S1 in the Supporting Information (SI)]. Metal nanoparticles (1−2 nm diameter) were prepared by chemical reduction (with $NaBH_4$) of the corresponding metal salts in the presence of peptide conjugate **1**, in a methanol/water mixture. In addition to TEM analysis, formation of the nanoparticles was confirmed by UV−vis absorption spectra, where weak (because of the small nanoparticle size) metal-dependent plasmonic bands were

[†] Dipartimento di Scienze Chimiche.
[‡] Dipartimento di Biologia.
[§] Dipartimento di Scienze Biomediche Sperimentali.
[||] CRIBI.

10.1021/ja107588q

observed (Figure S4). Ormosil nanoparticles (10−20 nm diameter) were prepared by ammonia-catalyzed polymerization of surfactant-stabilized microemulsions of vinyltriethoxysilane (VTES) in water and in the presence of peptide conjugate **2**.[14]

All of the nanoparticles prepared are fully soluble not only in water but also in alcoholic (methanol, ethanol) solvents. The peptide coating is so stable that the nanoparticles can be purified by reversed-phase HPLC, even using trifluoroacetic acid-containing eluents (Figures S5−S7).

Most importantly, circular dicroism (CD) analysis confirmed that the peptide chains retain a helix structure after nanoparticle grafting.[15] In particular, two negative bands at 225−227 nm (peptide n → π^* transition) and 206−208 nm (peptide $\pi \rightarrow \pi^*$ transition) that are typical of helix structures[16] were detected in the spectra of both the free peptide in water and the peptide-coated nanoparticles (Figure 1). Interestingly, the ratio of the intensities of the n → π^* and $\pi \rightarrow \pi^*$ bands (R) for the free peptide in water was 0.56 (Figure 1 and Figure S10), and the $\pi \rightarrow \pi^*$ band was centered at 206 nm; these values have been attributed to a significant population of concomitant 3_{10}- and α-helix conformations.[16] When the peptide was grafted onto the surface of Ag and Pt nanoclusters, the R values increased to 0.67 and 0.75, respectively, and a red shift in the $\pi \rightarrow \pi^*$ band was observed, indicating an increase in the amount of the α-helix structure. Finally, R values close to 1 (with the position of the $\pi \rightarrow \pi^*$ band reaching 208 nm) were detected in the case of Au and ormosil particles, as expected for a full α-helix structure of the peptide. Thermogravimetric analysis (TGA) (Figures S2 and S3) indicated that this trend is related to the packing of the peptides on the particle surfaces. In fact, in the case of Ag and Pt nanoparticles, the calculated peptide footprints were 0.11 and 0.12 nm^2, respectively, which are similar to the values reported for 2 nm gold nanoparticles coated with short peptides in the 3_{10}-helix conformation.[11a] In the case of Au and ormosil nanoparticles, the peptide footprints increased to 0.65 and 0.69 nm^2, respectively.[17]

Apparently, when they are grafted onto the nanoparticles, the peptides switch their conformation from the 3_{10}-helix to the bulkier α-helix, likely to achieve optimal packing on the nanoparticle surface. Interestingly, in the case of small (1−2 nm) gold nanoparticles coated with small 3_{10}-helix-forming peptides, it has been reported that the peptide density on the particle surface is not controlled by the peptide-to-metal ratio used in the synthesis.[11a] The results reported here may indicate that, on the contrary, the nature of the metal core could be crucial in determining the degree of peptide surface coverage and consequently the kind of helix structure assumed.

In addition to their ability to form 3_{10}-helices even in short sequences, Aib-rich peptides show several other intriguing properties. They are produced as secondary metabolites by several fungi and are characterized by antibacterial, antiviral, and antifungal activities, all of which are due to their ability to bind cell membranes and increase their permeability.[18] Moreover, the presence of C^{α}-tetrasubstituted α-amino acids makes these peptides highly resistant to proteolysis, which is crucial for the development of effective peptide-based drugs.[19] On this basis, nanoparticles coated by such peptides may present interesting biological properties.

An initial investigation of the interaction of these nanoparticles and biological systems was then performed by measuring their uptake by different cell lines, including both epithelial cancer cells (HeLa and A431) and cells from the immune system (human macrophages and primary blood monocytes). For these studies, we used 15 nm ormosil nanoparticles since they can be easily doped with fluorescent dyes without affecting either the photophysical properties of the latter or the surface of the nanoparticles.[14] A

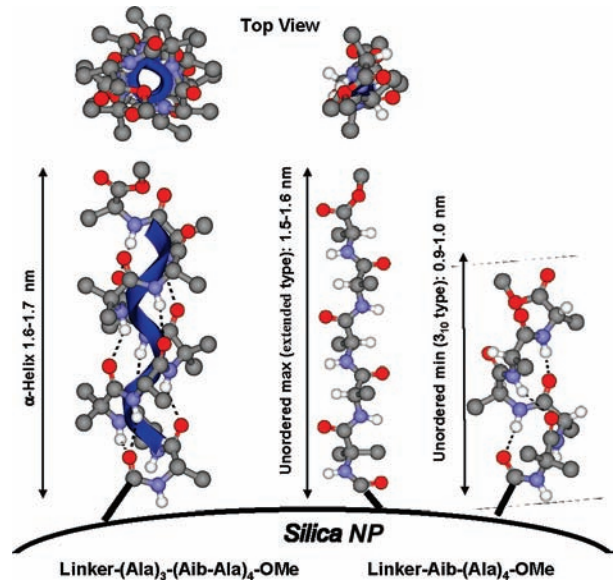

Figure 2. Lengths and footprints of ormosil nanoparticle-grafted peptides **2** (α-helix) and **3** (unordered with minimum and maximum possible lengths corresponding to the lengths of the 3_{10}-helix and the extended chain, respectively).

trialkoxysilane derivative of the cyanine dye CHROMIS 678-Z (**4**) (see the SI) was used to ensure covalent grafting of the dye to the silica network, thus preventing it from leaking out of the nanoparticles. Biological tests were simultaneously performed on dye-doped nanoparticles that were either uncoated or coated with either peptide−silane derivative **2** (Figure 1) or **3** (Figure 2). Derivative **3**, which is based on the pentameric sequence H-Aib-Ala$_4$-OMe, was selected as an unordered reference analogue of **2** on the basis of the following considerations: (i) the Aib-Ala$_4$ sequence grants water solubility, the maximum possible conservation of the residues present in **2**, and the inability to form helix structures (which is different from sequences with more Aib residues or with the Aib residue in a more central position); (ii) the length of the nanoparticle-grafted unordered **3** spans the range between those of the 3_{10}-helix and the extended (β-sheet like) conformation[20] and hence should be very similar to the length of **2** in the α-helix conformation (Figure 2). As expected, the CD spectrum of the **3**-coated ormosil nanoparticles (Figure S11) demonstrated that in these nanoparticles the grafted peptides are in an unordered conformation. Moreover, TGA analysis indicated that the footprint of **3** on the ormosil particles is 0.43 nm^2. This value is smaller than that of **2** on the same nanoparticles (0.69 nm^2; see above) and reflects well the lower bulkiness of the unordered conformation in comparison with the α-helix.

Dye-doped ormosil nanoparticles were incubated with the different cell lines for 6 h at 37 °C in culture medium containing fetal calf serum (FCS). Their uptake and acute toxicity effects were investigated by cytofluorimetry and confocal microscopy experiments. Neither the coated nor uncoated nanoparticles showed any acute toxicity to the cell lines investigated under the experimental conditions employed.

The results of the flow cytofluorimetric uptake analysis (Figure 3) are remarkable. Epithelial cells (HeLa, A431) associated to the different nanoparticles with a dose-dependent behavior related to the intrinsic uptake ability of the different cell lines but substantially independent of the features of the nanoparticle surface. On the contrary, association to human macrophages and monocytes was strongly dependent on the presence of the peptide coating on the nanoparticles. It is worth nothing that (i) these cells efficiently

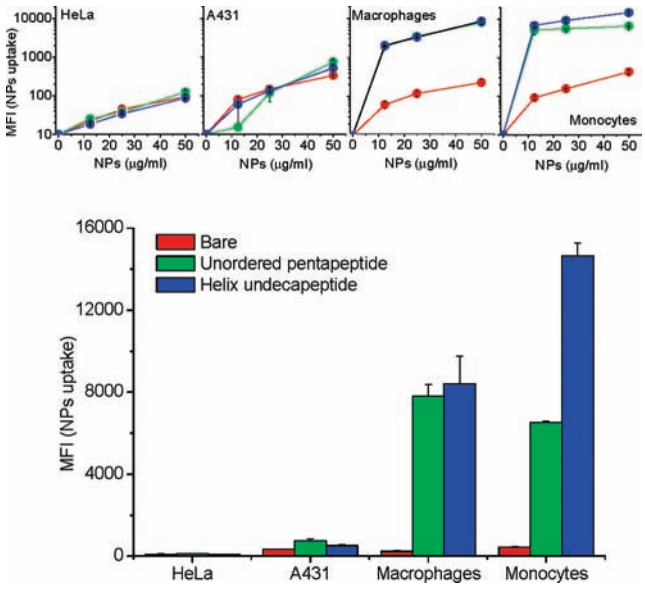

Figure 3. (top) Dose-dependent nanoparticle uptake by HeLa cells, A431 cells, macrophages, and monocytes treated with ormosil nanoparticles: (red) uncoated; (green) coated with the unordered pentapeptide; (blue) coated with the helix undecapeptide. Uptake is expressed as mean fluorescence intensity (MFI) as determined by cytofluorimetry. A logarithmic scale is used to allow a better appreciation of the trends for the single cell lines. (bottom) Comparison (linear scale) of the uptake of the different cell lines treated with the different nanoparticles (50 μg/mL) for 6 h at 37 °C.

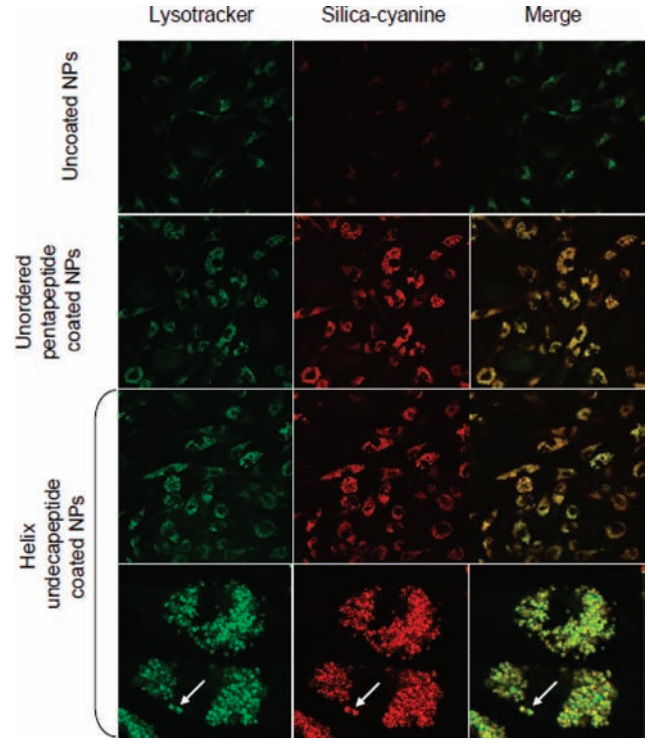

Figure 4. Confocal microscopy images showing the intracellular distribution of nanoparticles in human macrophages treated with the different nanoparticles (50 μg/mL) for 6 h at 37 °C. The left column shows the Lysotracker probe localization, the central column the localization of the nanoparticles, and the right column the superposition of the first two columns to highlight the colocalization. Arrows in the bottom-row panels, which show magnified details of the upper panels, point to selected examples of acidic endo/phagosomes loaded with helix peptide-coated nanoparticles.

internalize uncoated ormosil nanoparticles and (ii) surface functionalization with neutral hydrophilic molecules greatly decreases the uptake.[14b,21] Here, in the case of macrophages, the amount of peptide-coated nanoparticles internalized was up to 45-fold greater than that of the uncoated nanoparticles, irrespective of the peptide derivative present in the coating (Figure 3).

The results obtained with the monocytes are even more interesting. In this case, not only was the uptake of both of the peptide-coated nanoparticles still much more efficient than that of the uncoated ones, but also this cell line even appeared to be capable of recognizing the organization of the particle surface. Indeed, the particles coated with the helical undecapeptide **2** were taken up 2−3-fold more efficiently than those protected with the unordered pentapeptide **3**.

Confocal microscopy experiments (Figure 4) confirmed that the peptide-coated nanoparticles associate to macrophages much more effectively than do uncoated nanoparticles. Moreover, such an analysis demonstrated that virtually all of the cell-associated nanoparticles were engulfed and transported into the cell cytoplasm with a compartmentalized signal that tended to be distributed around the perinuclear region. High colocalization of the nanoparticle signals with the Lysotracker lysosome probe suggested that they were endocytosed and accumulated in acidic endolysosomal/phagosomal membrane compartments, as expected for this kind of cell. In contrast, but in full agreement with flow cytofluorimetry data, uncoated nanoparticles gave a very low fluorescence signal under these conditions, indicating relatively less efficient cell internalization.

In summary, we have de novo designed, synthesized, and characterized a new set of water-soluble nanoparticles coated with peptides in helix conformations. Apparently, the helix structure switches from the 3_{10}- to the α-helix conformation with decreasing peptide density on the nanoparticles. This is controlled either by the nature of the nanocrystal core (for metal nanoparticles) or the synthetic conditions (for ormosil nanoparticles). More importantly, we have found that these systems, which form a precise helical−spherical domain, have intriguing biological properties. Indeed, we observed that peptide-coated and uncoated nanoparticles associate to two cancer cell lines with the same efficacy, while the presence of the peptide induces a marked gain of uptake by monocytes and antigen-presenting macrophages. Such ability is strongly related to the biomimetic peptide coating and could be strengthened, in the case of monocytes, by the presence of an organized helix structure. Several factors, such as different surface features, hydrophobicity, and even specific recognition by cell-dependent receptors, may be the basis of this behavior, which will require further investigation. Possible applications of these properties range from the control of inflammatory phenomena and immune-system-related disorders to the development of immunization strategies. Such developments, as well as the behavior of peptide-coated nanoparticles based on Ag, Au, and Pt cores, are currently under investigation in our laboratories.

Acknowledgment. Financial support for this research was partly provided by the European Union (FP7, Grant 201031 NANOPHOTO). The authors thank Prof. C. Toniolo and Prof. P. Scrimin for encouragement and helpful discussions, F. Selvestrel for the synthesis of **4**, and E. Longo for help with chemical characterization.

Supporting Information Available: Experimental details and synthesis and characterization of the peptide ligands and the nanoparticles. This material is available free of charge via the Internet at http://pubs.acs.org.

References

(1) For example, see: Balzani, V.; Credi, A.; Venturi, M. *Chem.—Eur. J.* **2002**, *8*, 5524–5532.
(2) (a) Shenhar, R.; Rotello, V. M. *Acc. Chem. Res.* **2003**, *36*, 549–561. (b) Goesmann, H.; Feldmann, C. *Angew. Chem., Int. Ed.* **2010**, *49*, 1362–1395.
(3) (a) Templeton, A. C.; Wuelfing, M. P.; Murray, R. W. *Acc. Chem. Res.* **2000**, *33*, 27–36. (b) Daniel, M. C.; Astruc, D. *Chem. Rev.* **2004**, *104*, 293–346. (c) Gentilini, C.; Pasquato, L. *J. Mater. Chem.* **2010**, *20*, 1403–1412.
(4) (a) Prins, L. J.; Mancin, F.; Scrimin, P. *Curr. Org. Chem.* **2009**, *13*, 1050–1064. (b) Bonomi, R.; Selvestrel, F.; Lombardo, V.; Sissi, C.; Polizzi, S.; Mancin, F.; Tonellato, U.; Scrimin, P. *J. Am. Chem. Soc.* **2008**, *130*, 15744–15745. (c) Schatz, A.; Reiser, O.; Stark, W. J. *Chem.—Eur. J.* **2010**, *16*, 8950–8967.
(5) Bunz, U. H. F.; Rotello, V. M. *Angew. Chem., Int. Ed.* **2010**, *49*, 3268–3279.
(6) Imahori, H.; Fukuzumi, S. *Adv. Mater.* **2001**, *13*, 1197–1198.
(7) Nie, Z. H.; Petukhova, A.; Kumacheva, E. *Nat. Nanotechnol.* **2010**, *5*, 15–25.
(8) (a) Giljohann, D. A.; Seferos, D. S.; Daniel, W. L.; Massich, M. D.; Patel, P. C.; Mirkin, C. A. *Angew. Chem., Int. Ed.* **2010**, *49*, 3280–3294. (b) Boisselier, E.; Astruc, D. *Chem. Soc. Rev.* **2009**, *38*, 1759–1782.
(9) In a different but related application, peptide-coated water-soluble nanoparticles wherein the peptides are designed to fold in a helix structure under controlled conditions have been described. See: Aili, D.; Mager, M.; Roche, D.; Stevens, M. M. *Nano Lett.* [Online early access]. DOI: 10.1021/nl1024062. Published Online: Aug 26, 2010. Aili, D.; Mager, M.; Roche, D.; Stevens, M. M. *Chem. Soc. Rev.* **2010**, *39*, 3358–3370. Aili, D.; Enander, K.; Baltzer, L.; Liedberg, B. *Nano Lett.* **2008**, *8*, 2473–2478. Stevens, M. M.; Flynn, N. T.; Wang, C.; Tirrell, D. A.; Langer, R. *Adv. Mater.* **2004**, *16*, 915–918.
(10) (a) Pengo, P.; Baltzer, L.; Pasquato, L.; Scrimin, P. *Angew. Chem., Int. Ed.* **2007**, *46*, 400–404. (b) Levy, R.; Thanh, N. T. K.; Doty, R. C.; Hussain, I.; Nichols, R. J.; Schiffrin, D. J.; Brust, M.; Fernig, D. G. *J. Am. Chem. Soc.* **2004**, *126*, 10076–10084. (c) Pengo, P.; Broxterman, Q. B.; Kaptein, B.; Pasquato, L.; Scrimin, P. *Langmuir* **2003**, *19*, 2521–2524.
(11) (a) Fabris, L.; Antonello, S.; Armelao, L.; Donkers, R. L.; Polo, F.; Toniolo, C.; Maran, F. *J. Am. Chem. Soc.* **2006**, *128*, 326–336. (b) Holm, A. H.; Ceccato, M.; Donkers, R. L.; Fabris, L.; Pace, G.; Maran, F. *Langmuir* **2006**, *22*, 10584–10589. (c) Higashi, N.; Kawahara, J.; Niwa, M. *J. Colloid Interface Sci.* **2005**, *288*, 83–87. (d) Higuchi, M.; Nagata, K.; Abiko, S.; Tanaka, M.; Kinoshita, T. *Langmuir* **2008**, *24*, 13359–13363. (e) Schade, M.; Moretto, A.; Donaldson, P. M.; Toniolo, C.; Hamm, P. *Nano Lett.* **2010**, *10*, 3057–3061.
(12) (a) Karle, I. L.; Balaram, P. *Biochemistry* **1990**, *29*, 6747–6756. (b) Toniolo, C.; Crisma, M.; Formaggio, F.; Peggion, C. *Biopolymers* **2001**, *60*, 396–419.
(13) (a) Pavone, A.; Benedetti, E.; Di Blasio, B.; Pedone, C.; Santini, A.; Bavoso, A.; Toniolo, C.; Crisma, M.; Sartore, L. *J. Biomol. Struct. Dyn.* **1990**, *7*, 1321–1331. (b) Benedetti, E.; Di Blasio, B.; Pavone, V.; Pedone, C.; Santini, A.; Bavoso, A.; Toniolo, C.; Crisma, M.; Sartore, L. *J. Chem. Soc., Perkin Trans. 2* **1990**, 1824–1837.
(14) (a) Roy, I.; Ohulchanskyy, T. Y.; Pudavar, H. E.; Bergey, E. J.; Oseroff, A. R.; Morgan, J.; Dougherty, T. J.; Prasad, P. N. *J. Am. Chem. Soc.* **2003**, *125*, 7860–7865. (b) Rio-Echevarria, I. M.; Selvestrel, F.; Segat, D.; Guarino, G.; Tavano, R.; Causin, V.; Reddi, E.; Papini, E.; Mancin, F. *J. Mater. Chem.* **2010**, *20*, 2780–2787.
(15) The helix structure of the peptides grafted to the nanoparticles was further confirmed by ^{1}H NMR experiments performed on Au nanoparticles (Figures S8 and S9).
(16) (a) Formaggio, F.; Crisma, M.; Rossi, P.; Scrimin, P.; Kaptein, B.; Broxterman, Q. B.; Kamphuis, J.; Toniolo, C. *Chem.—Eur. J.* **2000**, *6*, 4498–4504. (b) Toniolo, C.; Polese, A.; Formaggio, F.; Crisma, M.; Kamphuis, J. *J. Am. Chem. Soc.* **1996**, *118*, 2744–2745.
(17) Peptide footprints for the ormosil nanoparticles were calculated by TGA analysis assuming a 1.5 g/cm^3 density of the ormosil core (see the SI).
(18) For example, see: Taira, J.; Shibue, M.; Osada, S.; Kodama, H. *Int. J. Pept. Res. Ther.* **2010**, *16*, 277–282, and references therein.
(19) De Zotti, M.; Biondi, B.; Formaggio, F.; Toniolo, C.; Stella, L.; Park, Y.; Hahm, K. S. *J. Pept. Sci.* **2009**, *15*, 615–619.
(20) Garcia, A. E. *Polymer* **2004**, *45*, 669–676.
(21) Tavano, R.; Segat, D.; Reddi, E.; Kos, J.; Rojnik, M.; Kocbek, P.; Iratni, S.; Scheglmann, D.; Colucci, M.; Rio-Echevarria, I. M.; Selvestrel, F.; Mancin, F.; Papini, E. *Nanomedicine* **2010**, *5*, 881–896.

JA107588Q